THE EFFECTS OF END TERMINATION ON THE ENDURANCE LIFE OF TWISTED STRING ACTUATORS

A Thesis

Presented to the faculty of the Department of Mechanical Engineering

California State University, Sacramento

Submitted in partial satisfaction of
the requirements for the degree of

MASTER OF SCIENCE

in

Mechanical Engineering

(Design and Dynamic Systems)

by

Bradley Scott Roan

FALL
2016

THE EFFECTS OF END TERMINATION ON THE ENDURANCE LIFE OF TWISTED STRING ACTUATORS

A Thesis

by

Bradley Scott Roan

Approved by:

___________________________________, Committee Chair
Akihiko Kumagai, Ph.D.

___________________________________, Second Reader
Kenneth S. Sprott, Ph.D.

____
Date

Student: Bradley Scott Roan

I certify that this student has met the requirements for format contained in the University format manual, and that this thesis is suitable for shelving in the Library and credit is to be awarded for the thesis.

____________________________, Graduate Coordinator _____________________
Akihiko Kumagai, Ph.D. Date

Department of Mechanical Engineering

Abstract

of

THE EFFECTS OF END TERMINATION ON THE ENDURANCE LIFE

OF TWISTED STRING ACTUATORS

by

Bradley Scott Roan

Actuation is possibly the most fundamental aspect of any robotic system; a robot without any means to interact with the physical world is simply a computer. As such, new actuation methods are valuable additions to the field of robotics, and optimization of such methods can help advance the field as a whole.

Twisted string actuators (TSA) are a relatively novel type of actuator, which convert the rotary motion of an electric motor to a tensile linear motion by twisting two or more strings around one another thereby shortening the length. When the twisting element is composed of high tensile strength fibers (such as high modulus polyethylene fiber), these actuators have the potential to possess many desirable characteristics of actuators, such as high force, high speed, high specific power (power to weight ratio), and high power density (power to volume ratio). Furthermore, because the transmission element is string, these actuators can be designed and built very cost efficiently.

One of the major drawbacks of TSAs is their endurance life. While many engineering components operate in the millions of cycles, twisted string actuators

operate in the range of tens of thousands of cycles. For some applications, this low endurance life is no issue, because the strings in the actuator are cheap and easily replaced. For many applications, however, this low of endurance life is unacceptable.

The purpose of this thesis is to explore the effects of the end termination of the twisted element on the endurance life of the actuator. The basic architecture and concept of twisted string actuators is presented, as well as the mathematical description of their behavior. A hypothesis concerning the endurance life of the twisted element with respect to the end termination of the twisted element is presented and supported. A potential solution to the problem of low endurance life of twisted string actuators is presented and tested alongside two other common architectures. The results from this test are presented and discussed.

When different architectures of twisted strings were tested and compared under identical conditions (i.e. style of string, material of string, resting length of twisting element, loading of the actuator, and actuation speed) it was found that the separator plate architecture outperformed both the pulley-to-pulley architecture, and the proposed architecture. The pulley-to-pulley tests resulted in a median endurance life of 36.5 cycles, the separator plate architecture resulted in a median endurance life of 364 cycles, and the proposed architecture resulted in a median endurance life of 115 cycles. During testing, the phenomenon of axial twist of individual strings, in addition to the twisting of the string pair driven by the motor, was observed, and identified as a potential explanation for the limited endurance life of the proposed architecture when compared with that of the separator plate architecture.

________________________, Committee Chair
Akihiko Kumagai, Ph.D.

____
Date

ACKNOWLEDGEMENTS

I would like to thank Professor Akihiko Kumagai for his enthusiasm for the subject I chose to research, and for guiding me towards a topic suitable for a graduate thesis. I would also like to thank him for being an accommodating advisor throughout my graduate experience at California State University Sacramento.

Next, I would like to thank Professor Kenneth S. Sprott, for his instruction in research methodology. This class taught me how to effectively conduct research on a graduate level, and gave me an introduction to the academic rigor of the mechanical engineering master's program. Without his instruction, I would not have known all the resources at my disposal for writing this thesis.

Finally, I would like to thank my wife, whose support and understanding never wavered during the long nights in the machine shop, the longer nights in the garage, and the endless hours in front of my computer.

TABLE OF CONTENTS

LIST OF TABLES

Tables Page

LIST OF FIGURES

Figures Page

Chapter 1. INTRODUCTION

Twisted string actuators are a novel type of actuator, used to convert the rotary motion of an electric motor into a tensile linear force. The force is produced by two or more strings twisting around one another, thereby shortening the length of the twisted bundle. In order for the bundle to twist and contract, one end must rotate with respect to the other, and one end must translate linearly with respect to the other. For the rotating end, most configurations employ a thrust bearing and a fixturing element such as a pulley to allow rotation but not translation. For the translating end, most embodiments of the actuator use a linear rail to guide the motion, but two different methods have been used to prevent the strings from rotating. The first: a plate with smooth holes that the strings pass through to allow linear motion, but prevent rotation past that point (this will be referred to as the separator method). The second: a fixturing element similar to that on the rotating end, is held by a linear bearing, which prevents it from rotating (this will be referred to as the pulley to pulley method).

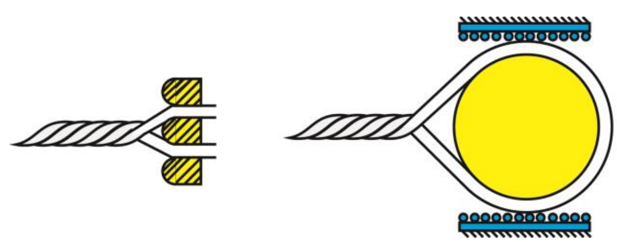

Figure 1: The two main types of twisted string architectures. The separator method (Left), and the pulley-to-pulley method (Right).

Although twisted string actuators have many desirable characteristics, they fall short of more conventional actuators such as hydraulics or ball screws in terms of endurance life. The purpose of this thesis is to identify why twisted string actuators have such limited endurance life, and attempt to provide a solution.

1.1 Literature Review

Twisted string actuators are a relatively new development; the earliest research cited in this paper was published in 2010. Due to the relative infancy of the technology, there are many aspects of it that remain to be researched and optimized. Many papers discuss the string behavior under twisting, as well as propose improved models to describe this behavior (Popov, 2013), however very little research exists concerning endurance life. Some papers discuss the cycles achieved in their design, ranging from 20,000 cycles (Gaponov, 2014) to 100,000 cycles (Palli, 2013), and even 400,000 cycles (May, 2010) for very low loads.

Few authors discuss the end termination of these designs, with most papers focusing on the system as a whole, and mentioning end termination briefly. Running the rope over a round element (pulley to pulley, as described in the introduction) at the ends was noted as being more promising than either tying or mechanical clamping of the string (Palli 2013), with a potential for 100,000 working cycles. This is supported by the report of only 20,000 cycles using a clamping method for the string (Gaponov, 2014).

It should be noted that Gaponov and Popov are often co-authors on papers concerning twisted string actuators. Anecdotally, the use of a separator architecture in (Popov, 2013), and the switch to a method closer to a pulley to pulley architecture, except with clamps as opposed to pulleys, in (Gaponov, 2014) might suggest that the research group identified pulley to pulley as being superior to the separator plate in terms of endurance life. However, this is pure speculation, and never explicitly stated.

In this thesis, the effects of end termination on endurance life are studied, and a method to optimize the endurance life via end termination is proposed. The proposed termination method is developed by contemplating the different loads induced by different termination methods, and verified by testing the proposed method alongside the other previously introduced methods

Chapter 2. TYPES OF ACTUATOR ARCHITECTURE

On a high level there are essentially two types of actuator architecture:

1) Fixed string quantity, where the amount of string in the twisted bundle remains the same. The pulley to pulley method is an example of this.
2) Variable string quantity, where more string is pulled into the bundle as twisting increases. The separator plate method is an example of this.

2.1 Fixed String Quantity

The fixed string quantity architecture (which is a term developed in this thesis, not widely used in this field of research), fixes the string bundle at both ends. One end is constrained linearly and allowed to rotate, the other end is constrained rotationally and allowed to translate. The term fixed string quantity is used because the amount of string in the twisting bundle remains unchanged throughout the stroke. Within this architecture, there are various methods for fixing the strings (Palli, 2013): wrapping the ends around pins or pulleys, mechanically clamping the strings, and tying the strings to posts. As can be seen in figure 1, most methods have common elements; they all use a motor to drive the mechanism, they all use thrust bearings to counteract the forces exerted on the rotary end, and they all have a linear bearing to guide the linear motion, and react the torque on the linear end.

Based on the findings from (Palli, 2013) the fixing method within this architecture which has the most potential for high endurance life is the one in which the string is allowed to wrap over a large diameter pin or pulley. The data in (Sloan, 2005), suggests that a

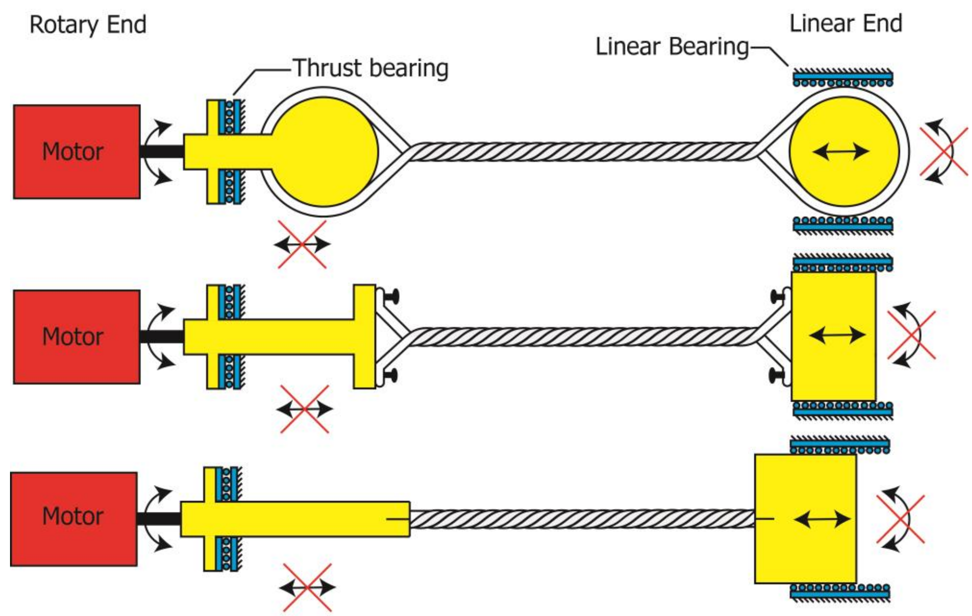

Figure 2: Three types of fixed string quantity actuators. Pulley to pulley, tied ends, and clamped ends.

larger diameter curvature improves endurance life in rope, which is corroborated by the industry guideline found in (Sampson Rope Technologies, 2014). It is for this reason that from the different options within this architecture, the pulley to pulley method has been selected for testing as a part of this thesis.

2.2 Variable String Quantity

The variable string quantity architecture fixes the string at only one end. Much like the fixed quantity architecture, variable string quantity actuators constrain one end of the string to rotary motion, supporting in linearly, with the string fixed in whatever way the designer of the actuator sees fit. The linear motion side of the actuator is where they differ; with the variable string quantity architecture, at the end of the twisted bundle, the string passes through a separator. The separator prevents the string from rotating, and allows it to pass through to the other side where it moves only linearly. This distinction was the inspiration for the naming of these two architectures: where fixed quantity actuators only have the quantity of string in the twisting bundle, variable quantity actuators draw string through the separator as they twist, adding more string to the twisted bundle. See figure 2 for a visual explanation of this architecture.

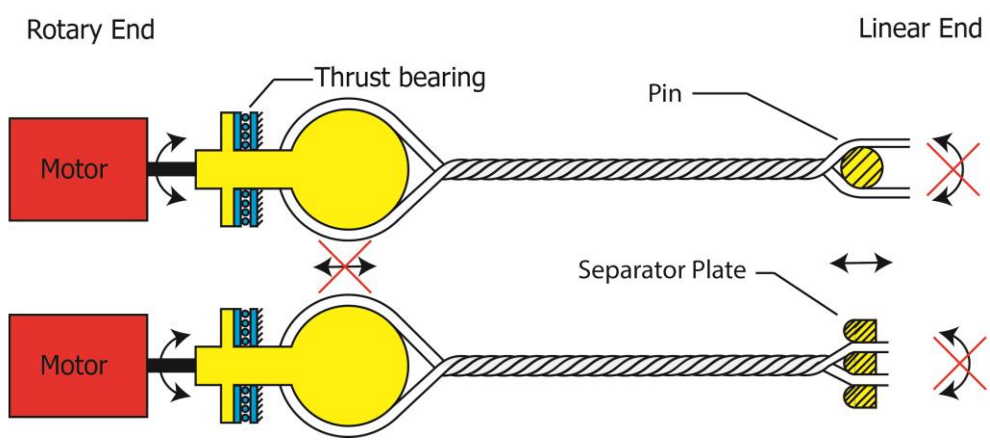

Figure 3: Two types of variable string quantity actuators. Pin method, and separator plate method.

The variable quantity architecture is much less prevalent in literature than the fixed quantity architecture, and is typically only used when the load on the actuator is applied in a manner where a flexible tensile element is necessary, as shown in (Popov, 2013), and can be seen in figure 4. The infrequent use of the variable quantity actuator style, despite its simpler construction (i.e. no need for bearings to react the torque of the motor), might suggest that the variable quantity architecture is inferior to the fixed quantity style, although no published literature states this.

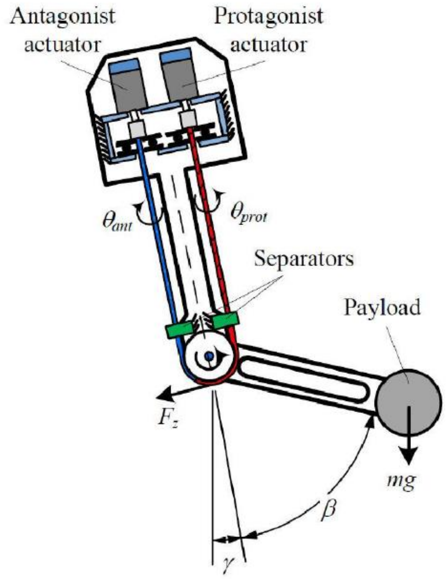

Figure 4: An example of the twisted pair being used as a flexible tensile element; passing through the separator, and wrapping around a pulley in order to produce torque.

The separator can be constructed of a smooth plastic such as Teflon to reduce sliding friction, or it could be as simple as a pin inserted into a plate perpendicular the direction of travel of the actuator. For the testing conducted in this thesis it has been determined that using a separator plate to separate the strings on the linear end of the actuator will be the most prudent course of action. A 3D printed plate made of ABS plastic is cheap, easily manufactured, and possesses a low coefficient of friction with other plastics.

Chapter 3. GOVERNING EQUATIONS

One of the interesting concepts of twisted string actuators is that the reduction ratio is non-constant: when untwisted, the force output is theoretically infinite, and the distance travelled per radian turn of the motor is infinitesimally small, conversely, at end of stroke the force output is greatly reduced, and the distance travelled per radian turn of the motor is significantly increased. (Shisheie, 2013) described the axial force developed by the bundle as

$$F = \frac{\tau L}{\theta r_{var}^2} \tag{1}$$

Where F is the force generated, τ is the output torque of the motor, L is the length of the untwisted bundle, θ is the number of turns of the bundle in radians, and r_{var} is the radius of the untwisted bundle (the radius of the bundle is variable and increases as θ increases, hence the "var" subscript). Notice that as θ goes to zero, the force approaches infinity. In (Popov, 2013) r_{var} is described by

$$r_{var} = r \cdot \sqrt{\frac{L+\Delta X}{L}} \tag{2}$$

Where ΔX is the difference between the resting length of the twisted bundle and the current length, and r is the radius of the untwisted bundle. In (Popov, 2013) ΔX is given as

$$\Delta X = L - \sqrt{L^2 + \theta^2 r_{var}^2} \tag{3}$$

As can be deduced from looking at equations 2 and 3, there is a bit of a cyclical relationship if θ is used as the input. The easier approach is to define the required actuation length ΔX, and use equation 2 and the rearranged equation 3 to derive θ

$$\theta = \sqrt{\frac{(\Delta X - L)^2 - L^2}{r_{var}^2}} \tag{4}$$

With these equations, the behavior of the strings is sufficiently defined to build a test fixture with which to test the endurance characteristics of the strings. A diagram illustrating the Pythagorean behavior of the actuators is featured in (Popov, 2013) and can be seen in figure 5.

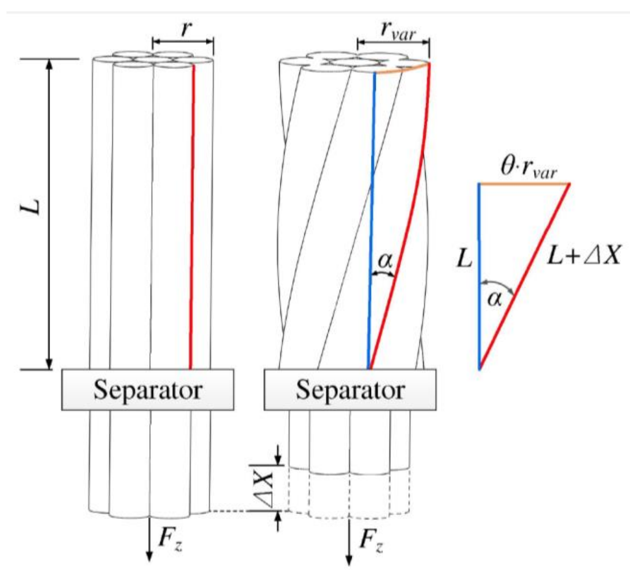

Figure 5: Illustration of the behavior of twisted strings.

Chapter 4. LOAD ANALYSIS OF STRINGS

By contemplating the geometry of the strings during the operation of a twisted string actuator, a loading analysis can be conducted, and predictions concerning the endurance life of different termination methods can be made. The nature of tensile elements only being able to support tensile loads (not bending or compression), means that it can be reasonably assumed that the load on the twisting strings is resolved in line with the strings themselves. Building on this assumption, a deeper understanding of the loading conditions induced by different termination styles can be gained.

4.1 Pulley to Pulley Method

A static analysis of the pulley to pulley method reveals that the geometry of the twisting string causes an increase in the loading of the string as the twist angle increases.

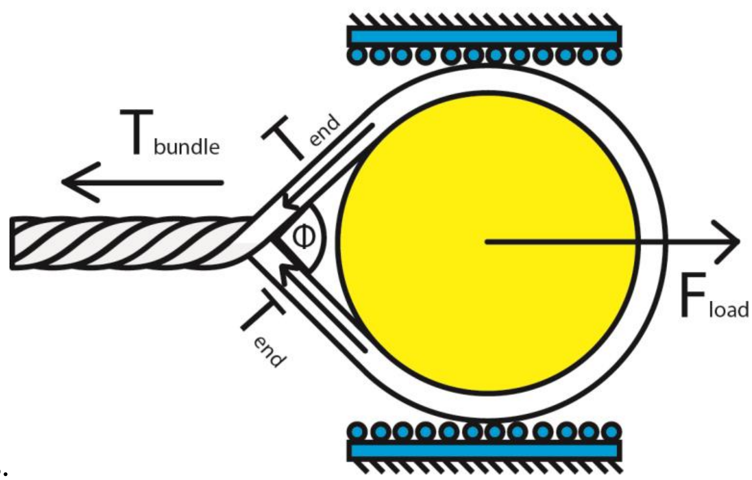

Figure 6: A static free body diagram of the pulley to pulley method

Based on the free body diagram shown in figure 6, it can be stated that:

$$T_{bundle} = F_{load} \tag{5}$$

Or, that the tension in the bundle is necessarily equal and opposite of the force of the load. Furthermore, it can be stated that the x direction components of the end segment tensions also sum to be equal and opposite of the force of the load:

$$2T_{end_x} = F_{load} \tag{6}$$

As the twisting of the bundle increased, so does the angle Φ, meaning that the x direction components of the end segment tensions contribute less to reacting the force of the load, and therefore the tension of the end segments necessarily increases as theta increases:

$$F_{Load} = 2T_{end} \cos\frac{\Phi}{2} \tag{7}$$

Becomes:

$$T_{end} = \frac{F}{2\cos\frac{\Phi}{2}} \tag{8}$$

This equation reveals that the end segment tension not only increases, but approaches infinity as Φ increases to 180 degrees. Because of this behavior, this fixturing method for twisted string actuators may produce tension in the end segments that is very close to the breaking strength of the string, which would lead to accelerated wear.

4.2 Separator Plate Method

A static analysis of the separator plate method reveals that in terms of loading of the strings, this method has superior qualities. Figure 7 shows that the end plate acts as a crude pulley, keeping the load in line with the axes of the end segments. This means that the tension in each end segment can be reduced to a capstan equation, whereas the axial tension of the bundle decreases as Φ increases.

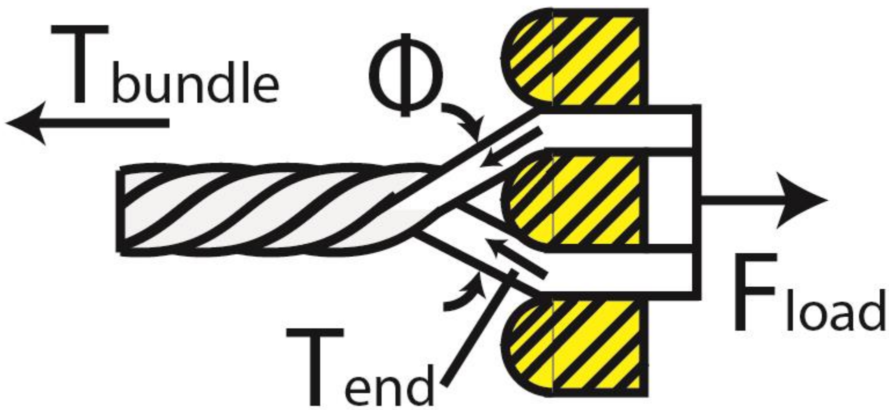

Figure 7: A static free body diagram of the separator plate method

Based on (Starkey 2011) the equation for the tension in the end segments is:

$$T_{end} = \frac{1}{2} F_{load} e^{\mu\omega} \quad (9)$$

Where μ is the kinetic friction coefficient between the separator plate and the string, and ω is the contact angle between the two in radians (which is equivalent to one half of Φ). The axial tension in the bundle is therefore:

$$T_{bundle} = 2T_{end}\cos(\frac{\Phi}{2}) \quad (10)$$

This shows that the force of the load staying in line with the end segments causes a decrease in the axial load of the bundle as theta approaches 180 degrees, and depending on the coefficient of friction between the string and the separator plate, the end segment tension may stay relatively low. It is important to note that as the tension in the bundle decreases, the load is increasingly reacted into the separator.

4.3 Discussion of existing Architectures

Based on (Sloan 2005), it can be stated that the endurance life of rope and string is significantly affected by the magnitude of loading it experiences during cycling. Furthermore, basic machine design knowledge reveals that a rolling interface between two components is superior to a sliding interface, from a wear perspective. Taking this, and the equations developed in the previous subchapters into account, a hypothesis concerning the endurance life of different twisted string architectures can be formed.

Assuming that the conditions of the test are the same: twisting element length, loading, actuation distance, and string material and construction are the same, it is proposed that the fixed length architecture (in this case the pulley-to-pulley fixturing method) would have inferior endurance life. The constant load on the bundle for the pulley-to-pulley method seems to be a non-issue, as the angle of the twisting string (α, in figure 5), is self limiting; geometrically, the alpha value can only grow so large before the strings begin resting on one another and preventing deeper twist. However, the angle Φ in figure 6, only starts limiting itself at 180 degrees, at which point the end segments experience a theoretically infinite load. Due to this fact, it is likely that the pulley-to-pulley architecture would be significantly limited in actuation length, as it can only be twisted until the end segments are loaded to their ultimate strength.

Conversely, the bundle of the separator plate method experiences an overall reduction in axial load, and given a low coefficient of friction between the strings and the separator plate, the load on the end segments only increases marginally with a 180 degree Φ angle (compared to the exponential growth of the pulley-to-pulley end segments). However, it should be noted that the separator plate method is not without drawbacks. For one, the radii on the holes of the separator plate are close in radius to the string itself, where most commercially available pulleys have a sheave diameter to rope diameter of at least 6. Furthermore, as previously discussed, sliding friction has a detrimental effect on endurance life, and the rope sliding through the separator plate is no exception. So, although it is proposed that the separator plate method will have superior endurance life to the pulley-to-pulley method, it is also proposed that a termination method without sliding friction or small string curvatures will be further superior.

4.4 Proposed Architecture

Due to the unfavorable string loading conditions in the pulley-to-pulley method, a prudent course of action would be to pursue an architecture that is without such limitations. Furthermore, although the loading conditions of the separator plate method are favorable, the sliding contact and small bend radii are not. It is for these reasons that the architecture (separator pulley method) shown in figure 8 is proposed.

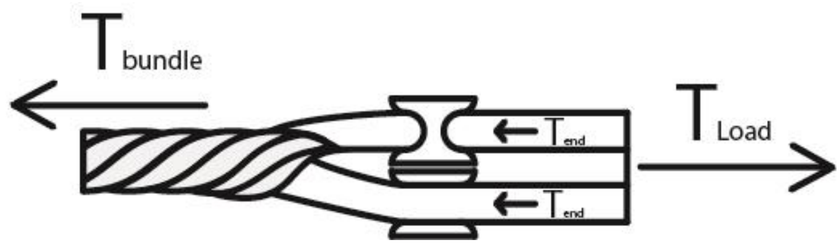

Figure 8: A static free body diagram of the proposed separation method

The proposed configuration emulates the separator plate method with rollers, so as to reduce sliding friction on the strings. The twisting bundle is split across two rollers which react the torque of the motor, and allow the strings to pass through to the load. A static analysis of this configuration shows the tension in the end segments is:

$$T_{end} = \frac{1}{2} T_{load} \tag{11}$$

The equations that govern this design are similar to that of the separator plate architecture, the tension in the bundle is governed by equation 10, however the tension in the end segments are subject to equation 11, not equation 9. Assuming increased endurance life over existing architectures, it might be considered an accomplishment for the weak point in the system to now be in the twisted bundle, as this would imply mediation of end termination weakness, and allow future research to focus on mediation of twisted bundle failure.

It is hypothesized that a rolling element separator will have superior endurance life to both the pulley-to-pulley method, and the separator plate method.

Chapter 5. DESIGN AND FABRICATION OF TEST FIXTURE

5.1 Mechanical Design

In order to test the hypotheses set forth in chapter 4, a test fixture was designed to cycle twisted string actuators until failure. Figures 9, 10, and 11 show a CAD model of the designed test fixture.

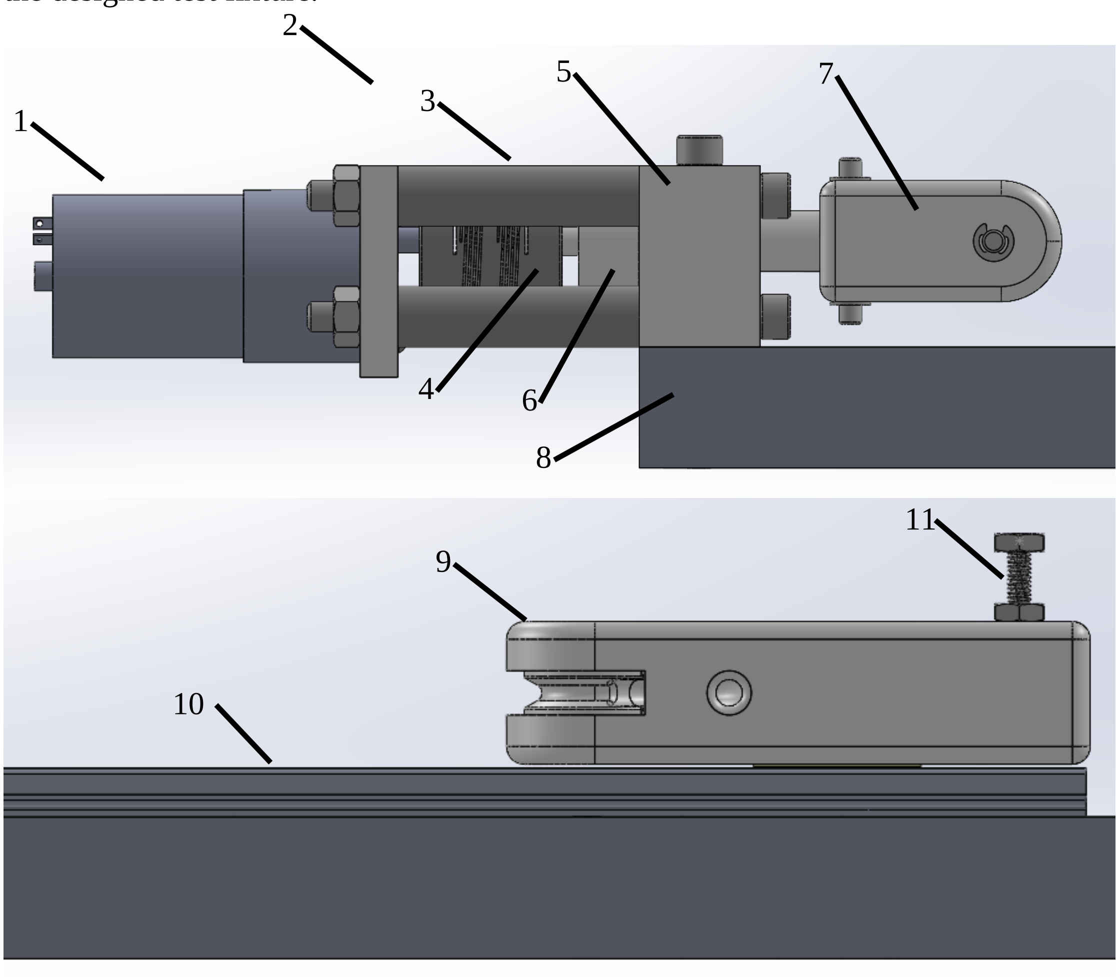

Figure 9: (1) DC gear motor, (2) Motor mount plate, (3) Spacers, (4) Shaft Coupling, (5) Bearing Plate, (6) Main Shaft, (7) Clevis, (8) Base Plate, (9) Carriage, (10) Linear Slide, (11) Eyelet Post

The motor is fixed to a plate, held off the bearing plate by spacers, and connected to the main shaft via a coupler, which allows axial, linear, and angular misalignment. The main shaft passes through the bearing block, which contains a roller thrust bearing, and a radial sleeve bearing (hidden). The main shaft is then connected to a clevis which houses a pulley, over which the string passes.

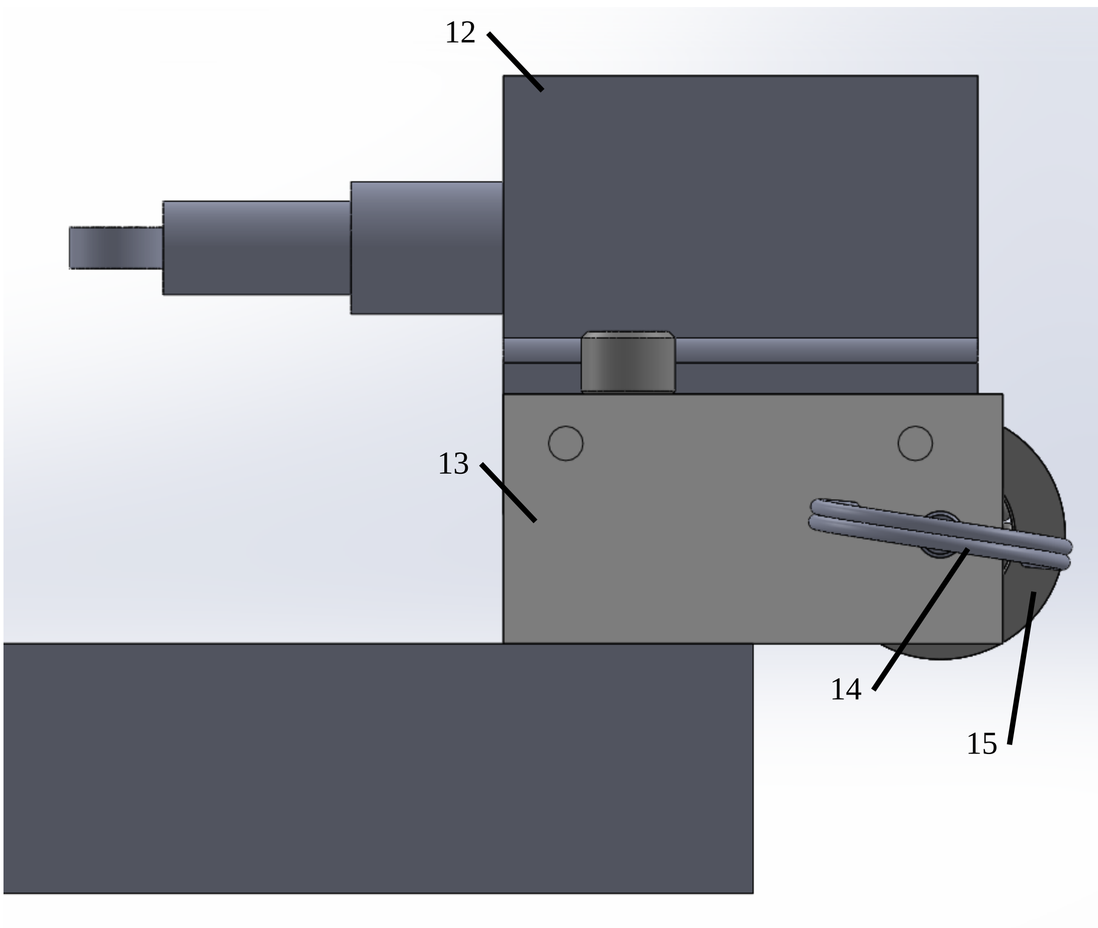

Figure 10: (12) String Potentiometer, (13) Load Redirection Plate, (14) Quick Release Pin, (15) pulley

This assembly is fixed to the base plate, and allows the string to be twisted, but not translate. Next, the strings are connected to the carriage, where they pass over a fixed pulley and through two holes where they are knotted, to prevent them from passing back through the holes. The carriage rides on a linear slide, and on top of the carriage is an eyelet post, which allows the carriage to be connected to a string potentiometer. Due to the linear slide, this assembly is allowed to translate linearly, but not rotate. A secondary string passed through a hole in the rear of the carriage, and out the top where it is knotted, preventing it from pulling back through. This string then goes on to the load redirection plate, where it passes over a pulley, which is held in place by a quick release pin. After being redirected downward by the pulley, this string is then tied to a 45 pound weight, which supplies the load for the test.

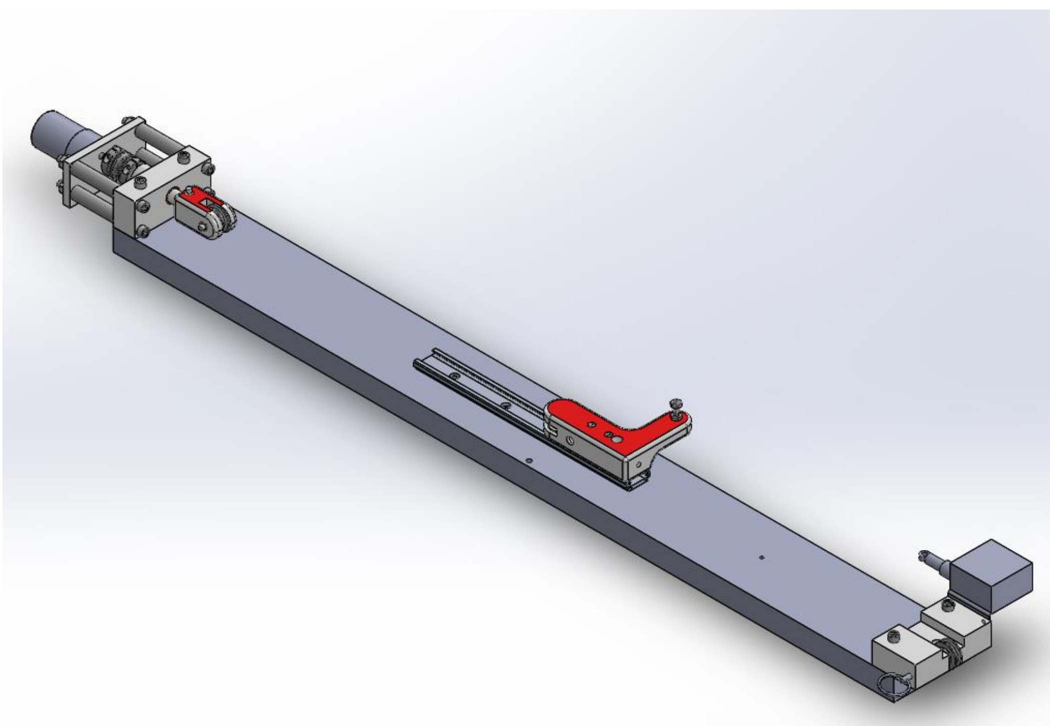

Figure 11: The pulley-to-pulley configuration of the test fixture

The motor mount plate, bearing block, carriage, and load redirection plate are all made of 3D printed ABS plastic, with any red surfaces shown indicating the face that was on the print bed. An assumption was made that 3D printed parts would be nearly as strong as a part machined out of the same material, as long as the load applied is not working to delaminate print layers from one another. Figure 12 and 13 show the same assembly, but with the separator plate, and separator pulley methods.

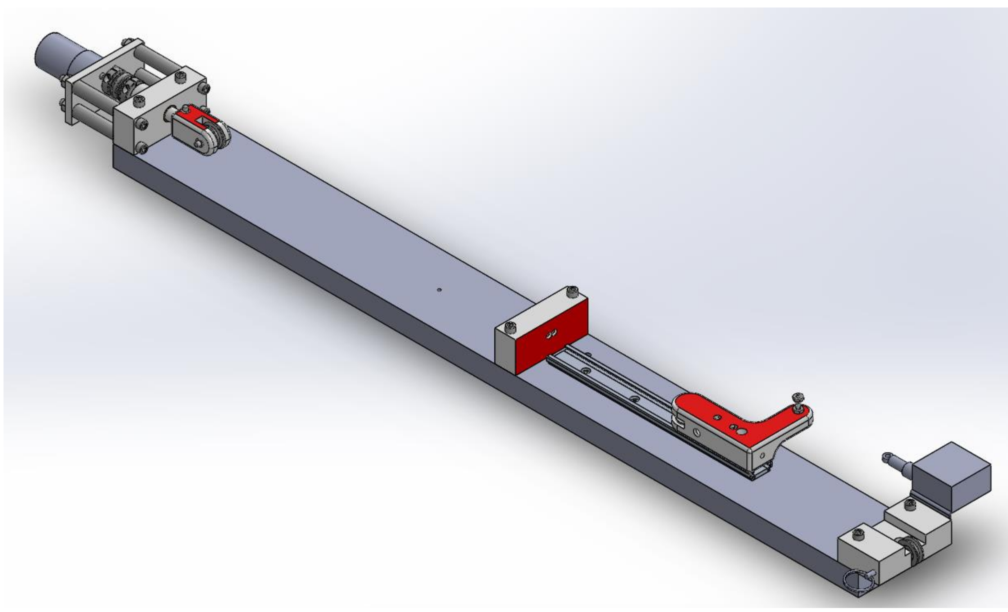

Figure 12: The separator plate architecture

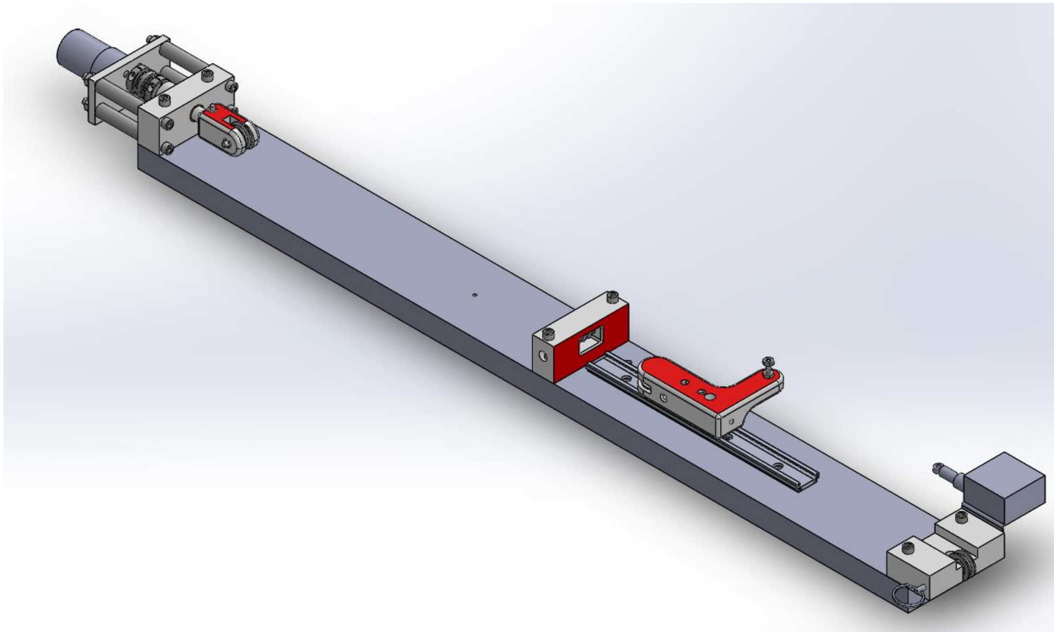

Figure 13: The separator pulley architecture

The separator plate, and separator pulley configurations of the test fixture are identical to the pully-to-pulley (figure 11) configuration, except that the linear rail is moved further towards the end of the base plate, and the strings pass through their respective separators before being attached to the carriage. The base plate was fabricated from a single bar of one inch thick aluminum, on a milling machine, after which various holes were tapped.

The design of the test fixture was driven by cost, ease of fabrication, and ease of assembly. Containing only one machined part, it is simple to fabricate, easy to assembly, and cost effective.

5.2 Electrical Design

The electrical components of the designed system consist of: A Raspberry Pi 2 model B+ microcomputer, an analog to digital chip that converts the analog signal of the

string potentiometer to a digital signal, and a driver which provides power to the motor. These components can be seen in figure 14. The Raspberry Pi was chosen because it has excellent processing power, 40 general purpose input/output pins, because it can save data directly to the onboard memory, and because the author is particularly well versed in Python, which is one of the programming languages the Raspberry Pi can interpret. Furthermore, whereas microcontroller programs are written in a development environment on a computer then uploaded onto the microcontroller, the Raspberry Pi can be programmed directly, with a keyboard and monitor. This direct programming results in faster development time. The analog to digital chip was needed because the Raspberry Pi is incapable of reading analog signals, and the MCP3008 is readily available, well documented, and is extremely cost effective. The analog to digital chip communicates with the Raspberry Pi via an SPI interface. The TB6612FNG motor driver was chosen because the raspberry pi is incapable of providing sufficient power to drive the motor selected for this application. The motor size was driven by the load conditions of the test (discussed in section 5.1), and the string diameter (to be discussed in chapter 6). The motor size then drove the specifications for the motor drive.

5.3 Design Analysis

In Order to ensure that the use of 3D printed ABS parts would be acceptable, finite element analysis was conducted on the load bearing elements of the test fixture. The full detail of the FEA analysis can be found in the appendices. Because 3D printed parts are not solid ABS, but a series of bonded filaments, it can be assumed that a 3D printed part will not perform identically to a solid machined ABS part; However, the Solidworks FEA cannot easily replicate the behavior of a 3D printed part. It is for this reason that a 3D printed tensile test sample was produced and tested against an FEA analysis. The test sample failed at 100.00 pounds, which was used as the benchmark force for the FEA test. The failed test sample can be seen in figure 15.

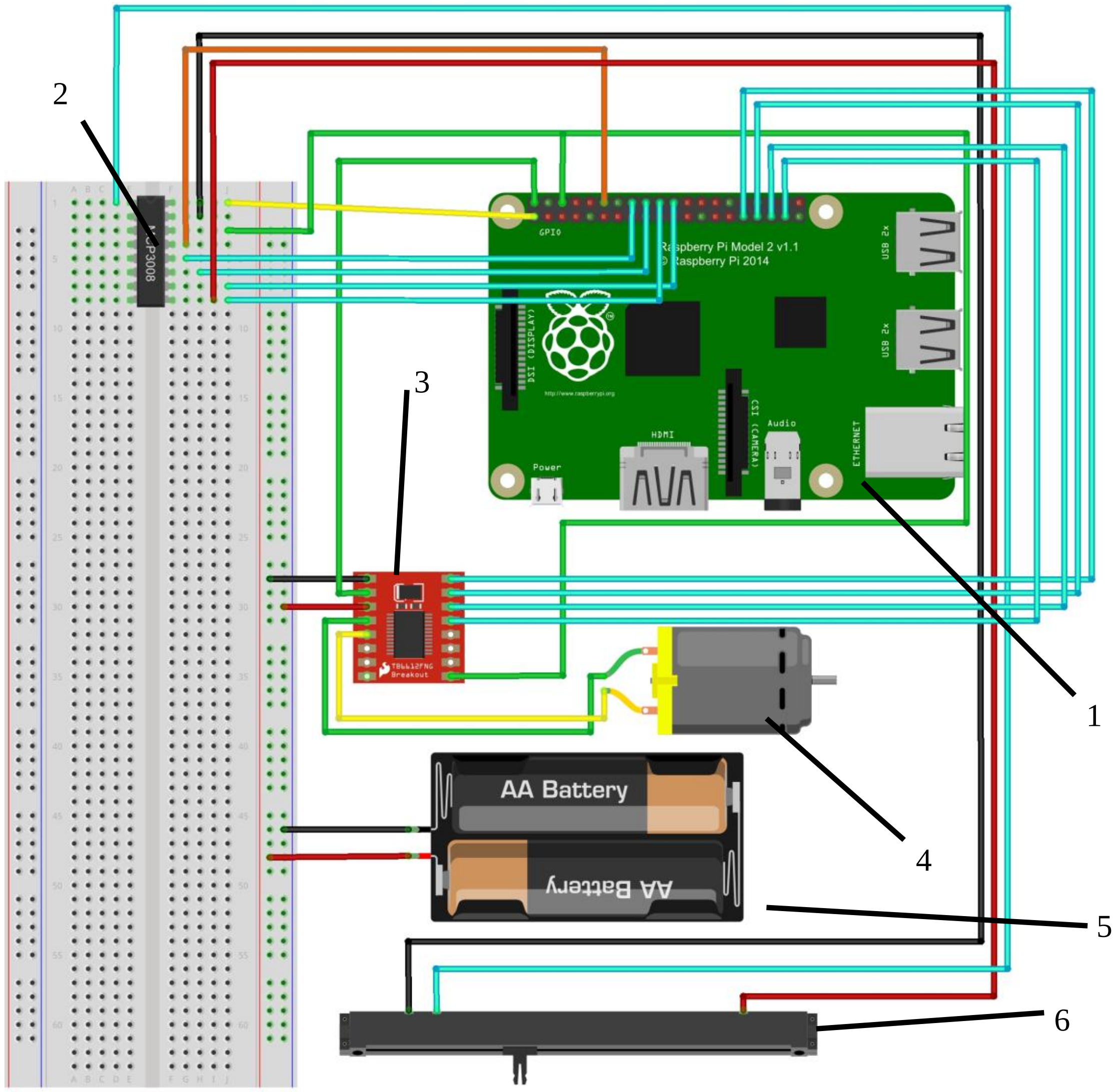

Figure 14: An electrical diagram of the control system. (1) Raspberry Pi Model 2 B+, (2) MCP3008 Analog to digital converter, (3) TB6612FNG Motor driver , (4) DC Gearmotor, (5)Power Supply (graphical stand-in for modified wall power supply), (6)String Potentiometer (Graphical stand-in)

Figure 15: The failed test sample

The FEA analysis of the test sample revealed that a maximum stress of 4568.6 PSI was developed, which resulted in a minimum factor of safety of 1.16. This factor of safety can be used to determine that 3D printed parts with proper layer orientation (i.e. the load is applied in a direction that is not delaminating the layers of the print), will fail at 86.2% of the load which would cause a solid machined part to fail. Figure 16 shows the stress distribution of the test sample, and figure 17 shows the factor of safety distribution.

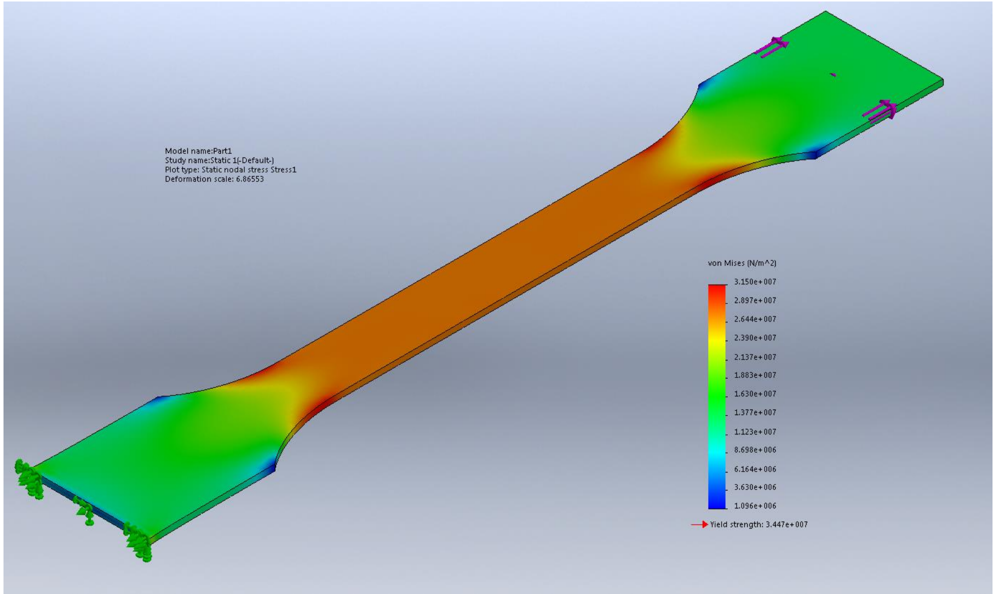

Figure 16: Test sample stress distribution

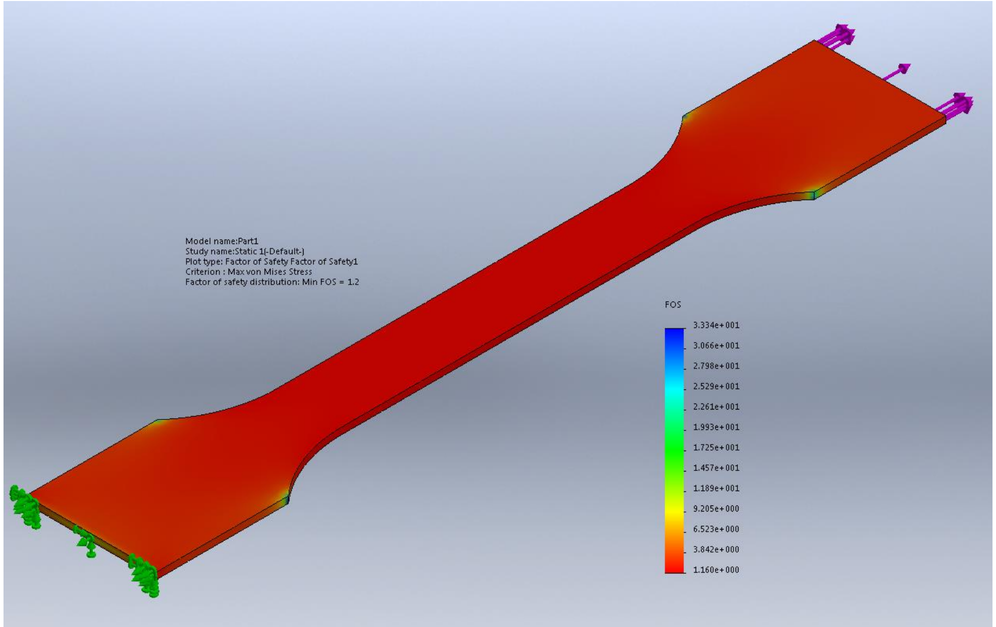

Figure 17: Test sample stress distribution

Chapter 6. TEST PROTOCOL

In order to ensure that the three different types of tests are valid and comparable, a test protocol must be established. First, the type of string to be tested has been chosen to be 1/8 inch diameter hollow braid polypropylene rope, which has a tensile strength of 100 pounds. This rope was purchased as a single 1,000 foot spool from Sunshine Cordage. Purchasing all the rope in a single spool was important, as it ensures uniform mechanical properties for all the rope used in the tests. Polypropylene rope was chosen over a stronger rope such as dyneema or spectra specifically because it has a much lower breaking strength; The low breaking strength of polypropylene means that the test can operate with low loads (in this case 45 pounds), with few cycles. As this test is designed to be comparative between end termination styles, as opposed to a endurance life optimization, low load and low cycles allow the individual tests to be conducted in quick succession.

The program that runs the tests was written in Python 3, and allows for 4 modes of operation: manual control, pulley-to-pulley, separator plate, and separator pulley. The full code can be found in the appendices. The explanation of the tests reference the variables set forth by figure 5, the steps of which are as follows:

1) The String is installed into the fixture.
2) Manual control is used to contract the actuator under full load to its maximum displacement until the string stops lengthening (approximately 3 cycles). This is a modification of the procedure found in (Gapanov 2014), which reduces

hysteresis, and leads to more consistent experimental results. It should be noted that (Gapanov 2014) underwent 50 cycles with resting periods between cycles, however it was manually observed in these experiments that lengthening of the strings stopped well before 50 cycles. This is most likely due to the use of much lower strength string material.

3) From a fully untwisted state ($\alpha = 0$, $L = 16$ inches) the string is twisted until the contraction length is equal to 25% (Tavkoli 2015) ($\Delta X = 4$ inches) of the original length of the twisting bundle. When the test is commenced the microcomputer creates a .txt file which specifies which test is being conducted, along with a timestamp of when the test started.

4) When the string reaches its full contraction length ($\Delta X = 4$ inches), the fixture reverses and unwinds the string until contraction length is 1% ($\Delta X \approx 0$ inches, $\alpha \approx 0$) of the resting length. The 1% has dual purpose: first, the contraction distance of the actuator is so low when the twist rotation is near zero that the string potentiometer and analog to digital chip don't have the resolution to accurately take the system to its original resting position. Second, it is theorized that going from a tightly wound bundle to a straight string produces undue strain on the strings, and that keeping the strings at least partially twisted helps reduce this strain. Steps 3 and 4 are repeated until the string breaks (which the microcomputer detects as described in step 6). The microcomputer writes each

cycle of the test to a micro SD card along with a time stamp of when the cycle was completed.

5) When the microcomputer registers that the test has been running for 3 minutes without completing a cycle, it stops the test, shuts down the motor, and saves the .txt file the data is saved in. The 3 minutes is indicative that either the string has broken, and thus the fixture cannot complete another cycle, or that something has gone wrong with the test. When the test is complete, the microcomputer also sends a text message to the author via the Twilio API, informing that the test is complete, and how many cycles have been completed. This mechanism to inform when tests are complete is a convenient way to ensure that tests are always running.
6) Each termination style will be run for a minimum of 10 tests.
7) After all tests have been completed, the data will be compiled and statistical analysis taken including: mean cycles for each termination style, median cycles for each termination style, and standard deviation for each termination style.

This test procedure will ensure that comparatively, the three termination styles tested will be equivalent, and the data collected from the tests will be valid. The data collected from these tests will either confirm or deny the hypotheses set forth earlier in this paper, and determine which, if any, is the superior termination style for twisted string actuators.

Chapter 7. RESULTS AND DISCUSSION

The data set forth in this chapter shows the results of the tests conducted. Table 1 shows the raw data collected from the tests, and figure 18 shows a graphical representation of the collected data.

Table 1: Test results, L and R indicate either a (L)inear end break, or a (R)otary end break. A linear end break being on the side of linear motion (separators or linear pulley), and a rotary end break being on the side of rotary motion (the motor)

Test Number	Pulley-to-pulley	Separator plate	Separator pulley
1	37 R	365 L	115 L
2	44 L	436 L	136 L
3	30 R	339 L	125 L
4	22 R	339 L	115 L
5	37 L	279 L	111 L
6	43 R	496 L	105 L
7	35 L	299 L	114 L
8	20 R	351 L	98 L
9	46 R	444 L	122 L
10	36 L	363 L	139 L
Mean	35	377.1	118
Median	36.5	364	115
STD	8.33	68.84	12.17

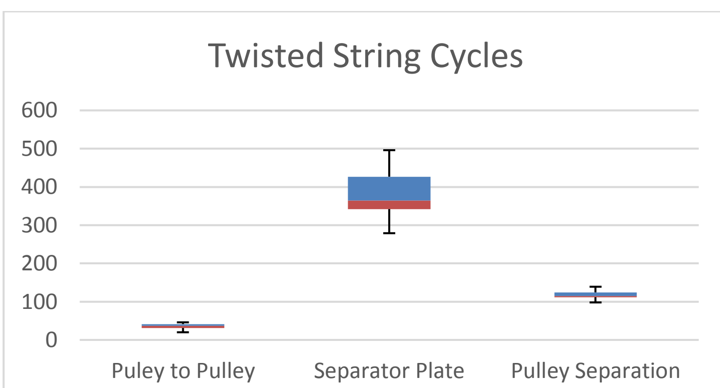

Figure 18: Test results

The collected data shows that the separator plate architecture is capable of a higher cycle count than both the pulley to pulley, and pulley separation architectures. It should be noted, however, that the data for the separator plate architecture also has a larger standard error than both the pulley to pulley and pulley separation architectures, indicating that there is a higher level of variability in the architecture.

This data validates the load analysis conducted earlier in the paper, showing objectively that the pulley to pulley architecture puts an increased load on both the end segments and the twisting bundle as compared to the separator plate method. Furthermore, the data validates the assumption that the tension in the end segments of the linear end versus the rotary end are roughly equal. The linear versus rotary end break rate of the pulley to pulley architecture is 40% to 60% respectively, indicating that the wear and stresses on either end is roughly equivalent. The separator plate architecture having a higher median cycle count, and ending every test with a break on the linear side validates two assumptions: 1) the curvature of the separator plate reduces the overall tension in the end segments to a value of half the applied load, and 2) the sliding friction of the separator plate results in increased wear on the strings.

Although the tests did validate the load analysis conducted earlier in the paper, the hypothesis set forth earlier in the paper was not supported by the collected data. However, due to the complexity of the string geometry and loading at the point of string separation, it would be imprudent to claim that this hypothesis is false. The more accurate claim to be made about the results of this test is that the designed rolling element separator results in inferior endurance life when compared to that of the separator plate architecture. There exists a potential for a better design of a rolling element separator which results in superior endurance life, the designed separator is simply not this one. Figure 19 shows an in-depth loading diagram for a string passing through a rolling element separator.

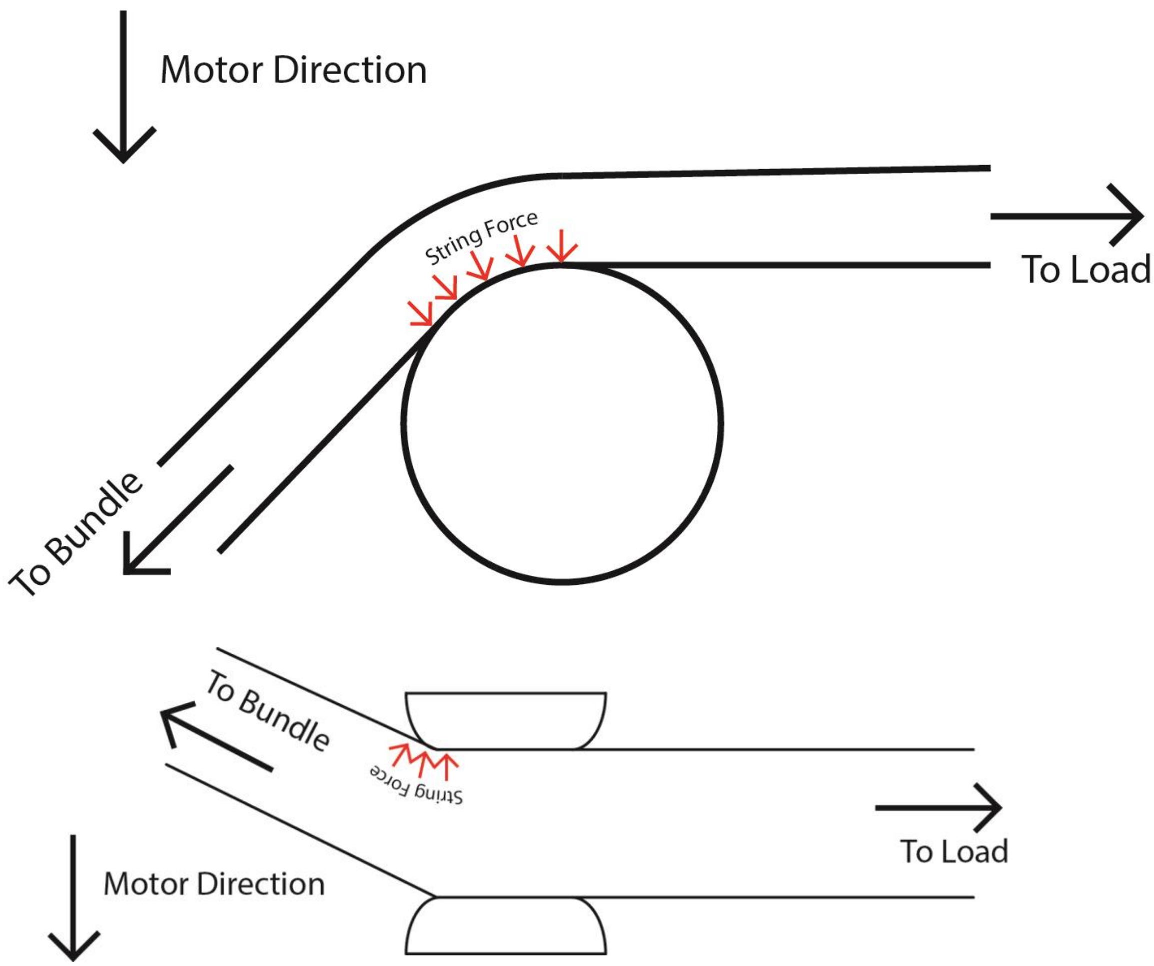

Figure 19: Above, side view of string passing over roller. Below, Top View of string passing over roller.

As can be seen in figure 19, the string not only applies an inward force to the pulley, as is typical with a string passing over a pulley, but also a side load, which pulleys are not meant to accommodate. These forces are the result of the pulley reacting the torque from the motor, as well as being held taught by the load. Furthermore, while testing a new phenomenon was observed: the strings not only travel linearly while being pulled into the twisting bundle, the two strings twist on their individual axes as they pass over the pulley. This axial twisting behavior is not accommodated by the pulley at all, and results in sliding friction on the string. Finally, as seen in figure 19, the strain on the rope is bidirectional. This alternating bidirectional strain likely causes increased wear on the strings when compared to the separator plate method, where the string is able to find a low energy state, resulting in a single constant strain. It is likely for these reasons that the rolling element separator did not have an endurance life comparable to that of the separator plate, and it is proposed that if a rolling element separator were designed to accommodate this complex string behavior and geometry, it would have a superior endurance life.

Chapter 8. CONCLUSION AND FUTURE WORK

In this thesis, analysis of existing work helps to identify the two most commonly used end termination architecture for twisted string actuators. Analysis of these common end termination architectures resulted in a hypothesis regarding which would perform best in terms of endurance life, and a third architecture was proposed to further improve upon endurance life. Using the equations governing twisted string actuators, a test fixture was designed and built to test different loading conditions, and clear results confirmed the hypothesis concerning existing end termination architectures, while the hypothesis concerning the proposed end termination was not confirmed, but also not fully refuted. Further analysis, explained potential reasons why the proposed architecture did not outperform both of the conventional end termination architectures.

Endurance of repeated stress systems is a highly complex and in depth field, and this research is only one facet of the aspects that could contribute to improve endurance life of twisted string actuators. Potential future work could include lubrication, woven versus twisted strings, materials, heat dissipation, motor speeds, and so on.

The robotics industry is a rapidly expanding and advancing market, and novel forms of actuation are constantly being sought. Twisted string actuators provide numerous advantages over traditional actuation methods, at the cost of endurance life, but with further work in the field, a deeper understanding of the phenomena surrounding the actuators can be achieved and endurance life can be improved.

Appendix A: Python Program

```
#!/usr/bin/env python

import time
import os
import RPi.GPIO as GPIO
import datetime
from twilio.rest import TwilioRestClient

GPIO.setmode(GPIO.BCM)
GPIO.setwarnings(False)
DEBUG = 1
client =
TwilioRestClient(account='AC81be36254e3d9b95ecdf4412fefb4fad',
token='00f0517ef46a3885839cce1fba7aaad7')

# read SPI data from MCP3008 chip, 8 possible adc's (0 thru 7)
def readadc(adcnum, clockpin, mosipin, misopin, cspin):
        if ((adcnum > 7) or (adcnum < 0)):
                return -1
        GPIO.output(cspin, True)

        GPIO.output(clockpin, False)  # start clock low
        GPIO.output(cspin, False)     # bring CS low

        commandout = adcnum
        commandout |= 0x18  # start bit + single-ended bit
        commandout <<= 3    # we only need to send 5 bits here
        for i in range(5):
                if (commandout & 0x80):
                        GPIO.output(mosipin, True)
                else:
                        GPIO.output(mosipin, False)
                commandout <<= 1
                GPIO.output(clockpin, True)
                GPIO.output(clockpin, False)

        adcout = 0
        # read in one empty bit, one null bit and 10 ADC bits
        for i in range(12):
                GPIO.output(clockpin, True)
                GPIO.output(clockpin, False)
                adcout <<= 1
                if (GPIO.input(misopin)):
                        adcout |= 0x1

        GPIO.output(cspin, True)

        adcout >>= 1       # first bit is 'null' so drop it
        return adcout
```

```
# change these as desired - they're the pins connected from the
# SPI port on the ADC to the Cobbler
SPICLK = 18
SPIMISO = 23
SPIMOSI = 24
SPICS = 25

# set up the SPI interface pins
GPIO.setup(SPIMOSI, GPIO.OUT)
GPIO.setup(SPIMISO, GPIO.IN)
GPIO.setup(SPICLK, GPIO.OUT)
GPIO.setup(SPICS, GPIO.OUT)
GPIO.setup(6, GPIO.OUT)
GPIO.setup(13, GPIO.OUT)
GPIO.setup(19, GPIO.OUT)
GPIO.setup(26, GPIO.OUT)

# 10k trim pot connected to adc #0
potentiometer_adc = 0;

last_read = 0       # this keeps track of the last potentiometer value
tolerance = 5       # to keep from being jittery we'll only change
                    # volume when the pot has moved more than 5
'counts'
print('Mode Selection:')
print('1)Manual control')
print('2)Separator plate')
print('3)Pulley Separation')
print('4)Pulley to pulley (short)')
mode_select = input('Please Select Mode:')

if mode_select == '1':
    while True:
        manualcontrol = input("Select Direction,(f)orward, (r)everse,
(s)top, (q)uit :")

        if manualcontrol == "f":
            GPIO.output(6, 1)
            GPIO.output(13, 0)
            GPIO.output(19, 1)
            GPIO.output(26, 1)
        if manualcontrol == "r":
            GPIO.output(6, 1)
            GPIO.output(13, 1)
            GPIO.output(19, 0)
            GPIO.output(26, 1)
        if manualcontrol == "s":
            GPIO.output(6, 1)
            GPIO.output(13, 0)
            GPIO.output(19, 0)
```

```
            GPIO.output(26, 1)
        if manualcontrol == "q":
            GPIO.output(6, 1)
            GPIO.output(13, 0)
            GPIO.output(19, 0)
            GPIO.output(26, 1)
            quit()

if mode_select == '2':
    print('Working...')
    setpoint = readadc(potentiometer_adc, SPICLK, SPIMOSI, SPIMISO,
SPICS)
    prevtrim_pot = setpoint
    advance = True
    counter2 = 0
    ts = time.time()
    currentday = datetime.datetime.fromtimestamp(ts).strftime('%Y-%m-
%d %H:%M:%S')
    file2 = open('SP '+currentday+'.txt', 'a')
    settime = time.time()
    while True:
        ts = time.time()
        trim_pot = readadc(potentiometer_adc, SPICLK, SPIMOSI,
SPIMISO, SPICS)
        if abs(trim_pot-prevtrim_pot)<10:
            prevtrim_pot = trim_pot
        if advance == True:
            GPIO.output(6, 1)
            GPIO.output(13, 0)
            GPIO.output(19, 1)
            GPIO.output(26, 1)
        if advance == False:
            GPIO.output(6, 1)
            GPIO.output(13, 1)
            GPIO.output(19, 0)
            GPIO.output(26, 1)
        if advance == True and prevtrim_pot > (setpoint+160):
            advance = False
            counter2 = counter2 + 1
            settime = time.time()
            timestamp2 =
datetime.datetime.fromtimestamp(ts).strftime('%Y-%m-%d %H:%M:%S')
            file2.write(timestamp2+'\n')
            file2.write('Current cycles: ' + str(counter2)+'\n')
            print(timestamp2)
            print('Current cycles: ' + str(counter2))
        if advance == False and prevtrim_pot < (setpoint+10):
            advance = True
        if ts > (settime + 300):
            GPIO.output(6, 1)
```

```
            GPIO.output(13, 0)
            GPIO.output(19, 0)
            GPIO.output(26, 1)
            file2.close()
            client.messages.create(to='+19092049283',
from_='+19513823386', body="Test Complete:"+str(counter2)+"cycles")
            quit()
if mode_select == '3':
    print('Working...')
    setpoint = readadc(potentiometer_adc, SPICLK, SPIMOSI, SPIMISO,
SPICS)
    prevtrim_pot = setpoint
    advance = True
    counter2 = 0
    ts = time.time()
    currentday = datetime.datetime.fromtimestamp(ts).strftime('%Y-%m-
%d %H:%M:%S')
    file2 = open('PS '+currentday+'.txt', 'a')
    settime = time.time()
    while True:
        ts = time.time()
        trim_pot = readadc(potentiometer_adc, SPICLK, SPIMOSI,
SPIMISO, SPICS)
        if abs(trim_pot-prevtrim_pot)<20:
            prevtrim_pot = trim_pot
        if advance == True:
            GPIO.output(6, 1)
            GPIO.output(13, 0)
            GPIO.output(19, 1)
            GPIO.output(26, 1)
        if advance == False:
            GPIO.output(6, 1)
            GPIO.output(13, 1)
            GPIO.output(19, 0)
            GPIO.output(26, 1)
        if advance == True and prevtrim_pot > (setpoint+160):
            advance = False
            counter2 = counter2 + 1
            settime = time.time()
            timestamp2 =
datetime.datetime.fromtimestamp(ts).strftime('%Y-%m-%d %H:%M:%S')
            file2.write(timestamp2+'\n')
            file2.write('Current cycles: ' + str(counter2)+'\n')
            print(timestamp2)
            print('Current cycles: ' + str(counter2))
        if advance == False and prevtrim_pot < (setpoint+10):
            advance = True
        if ts > (settime + 300):
            GPIO.output(6, 1)
            GPIO.output(13, 0)
            GPIO.output(19, 0)
```

```
            GPIO.output(26, 1)
            file2.close()
            client.messages.create(to='+19092049283',
from_='+19513823386', body="Test Complete:"+str(counter2)+"cycles")
            quit()
if mode_select == '4':
    print('Working...')
    setpoint = readadc(potentiometer_adc, SPICLK, SPIMOSI, SPIMISO,
SPICS)
    set_inches = 24.112 - (0.01869 * setpoint)
    prevtrim_pot = setpoint
    advance = True
    counter2 = 0
    ts = time.time()
    currentday = datetime.datetime.fromtimestamp(ts).strftime('%Y-%m-
%d %H:%M:%S')
    file2 = open('P2PS '+currentday+'.txt', 'a')
    settime = time.time()
    while True:
        ts = time.time()
        trim_pot = readadc(potentiometer_adc, SPICLK, SPIMOSI,
SPIMISO, SPICS)
        if abs(trim_pot-prevtrim_pot)<10:
            prevtrim_pot = trim_pot
            previnches = 24.112-(0.01869 * prevtrim_pot)
        if advance == True:
            GPIO.output(6, 1)
            GPIO.output(13, 0)
            GPIO.output(19, 1)
            GPIO.output(26, 1)
        if advance == False:
            GPIO.output(6, 1)
            GPIO.output(13, 1)
            GPIO.output(19, 0)
            GPIO.output(26, 1)
        if advance == True and previnches < (set_inches - (set_inches
* .175)):
            advance = False
            counter2 = counter2 + 1
            settime = time.time()
            timestamp2 =
datetime.datetime.fromtimestamp(ts).strftime('%Y-%m-%d %H:%M:%S')
            file2.write(timestamp2+'\n')
            file2.write('Current cycles: ' + str(counter2)+'\n')
            print(timestamp2)
            print('Current cycles: ' + str(counter2))
        if advance == False and previnches > (set_inches - (set_inches
* .0011875)):
            advance = True
        if ts > (settime + 300):
            GPIO.output(6, 1)
```

```
            GPIO.output(13, 0)
            GPIO.output(19, 0)
            GPIO.output(26, 1)
            file2.close()
            client.messages.create(to='+19092049283',
from_='+19513823386', body="Test Complete:"+str(counter2)+"cycles")
            quit()
try:
    main()
except KeyboardInterrupt:
    GPIO.cleanup()
```

Appendix B: Finite Element Analysis

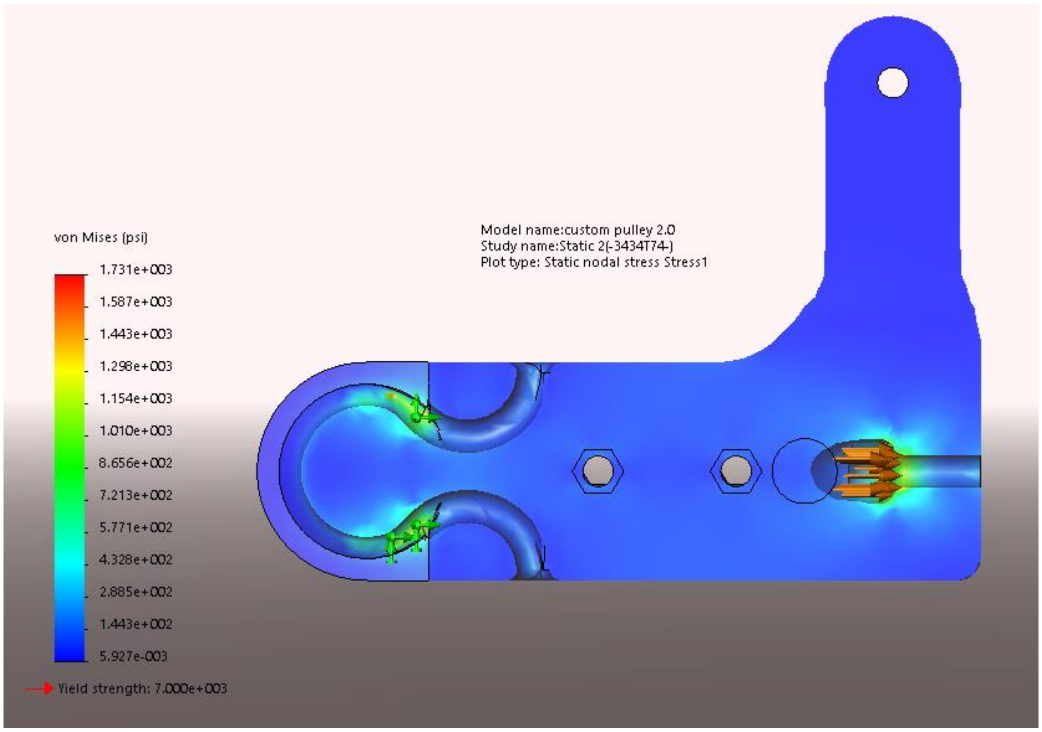

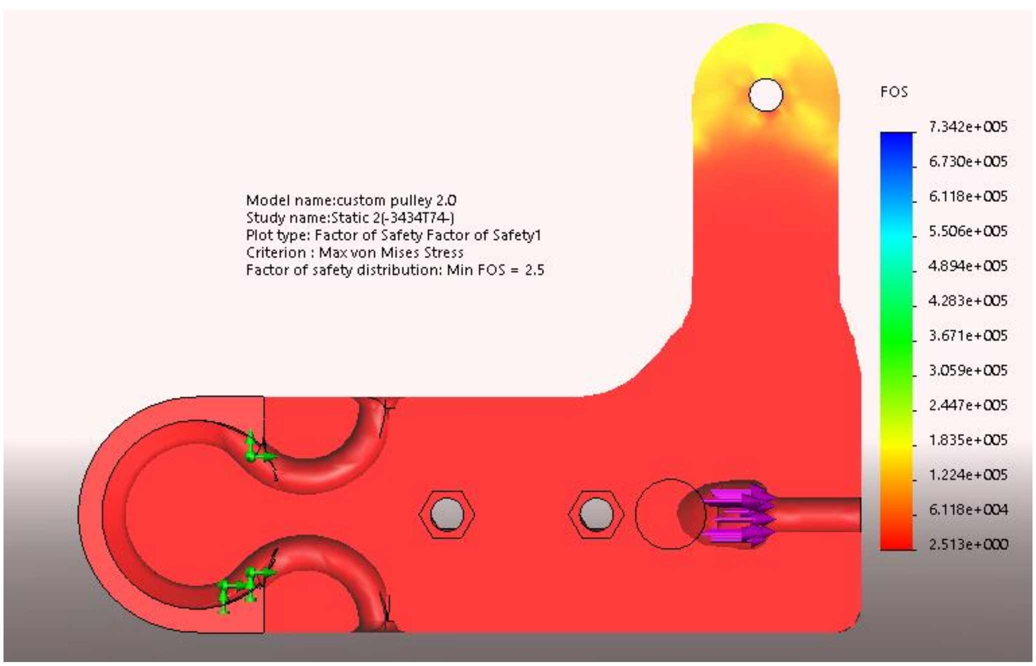

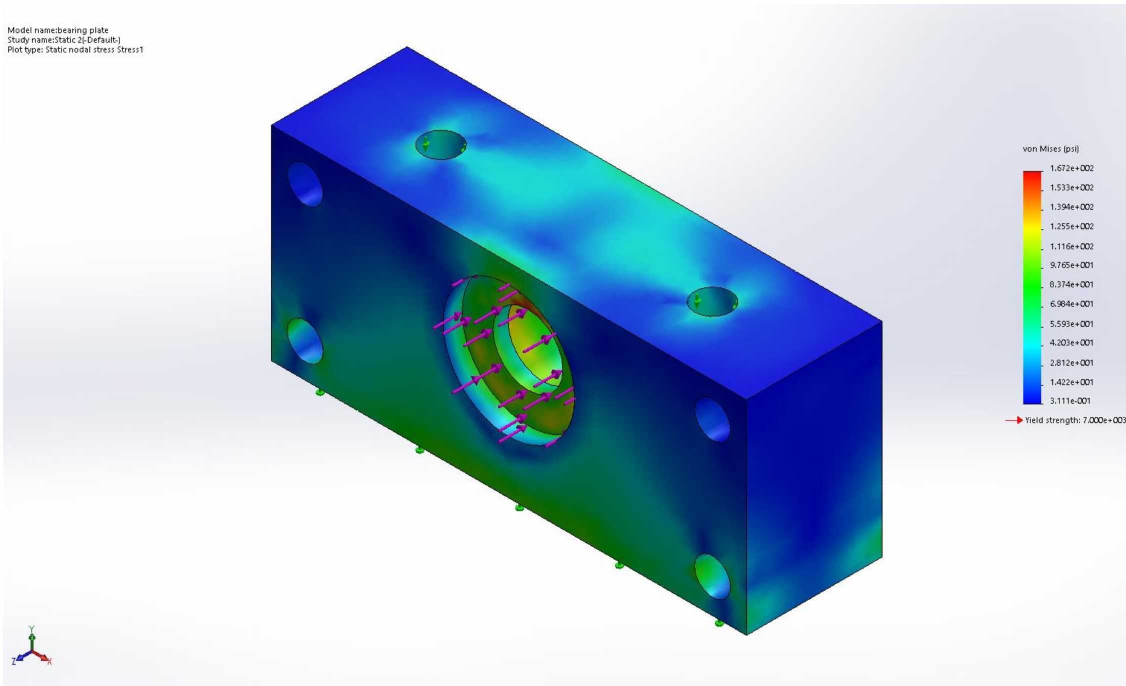
Model name:bearing plate
Study name:Static 2(-Default-)
Plot type: Static nodal stress Stress1
von Mises (psi)
1.672e+002
1.533e+002
1.394e+002
1.255e+002
1.116e+002
9.765e+001
8.374e+001
6.984e+001
5.593e+001
4.203e+001
2.812e+001
1.422e+001
3.111e-001
Yield strength: 7.000e+003
Y
Z
X

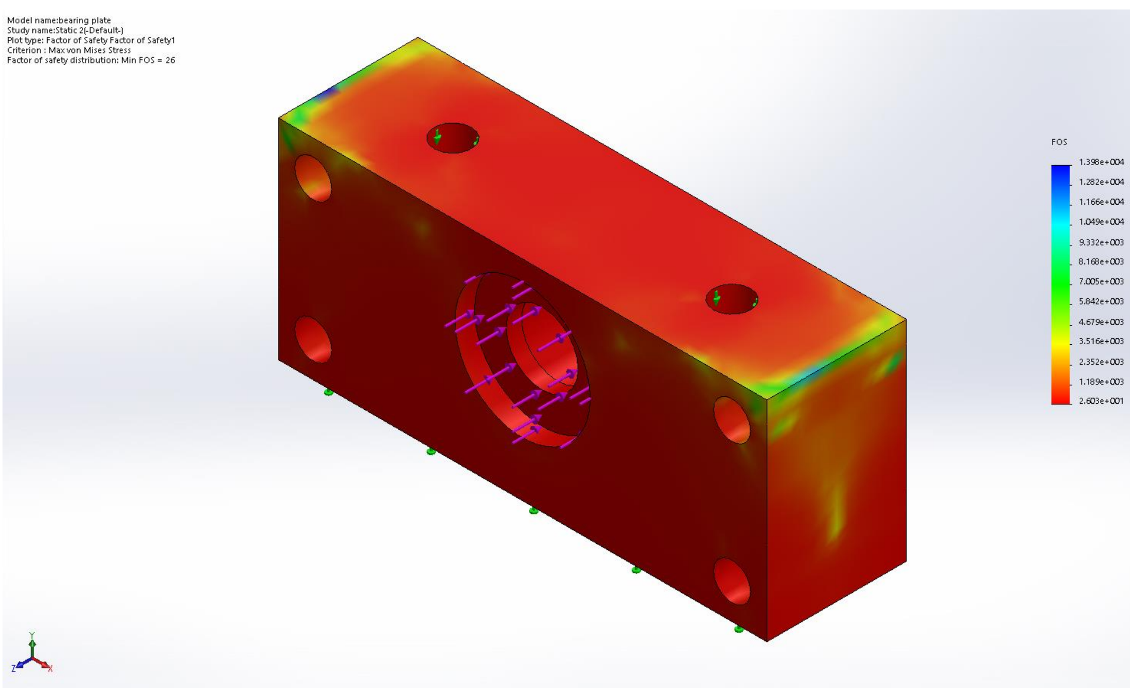
Model name:bearing plate
Study name:Static 2(-Default-)
Plot type: Factor of Safety Factor of Safety1
Criterion : Max von Mises Stress
Factor of safety distribution: Min FOS = 26
FOS
1.398e+004
1.282e+004
1.166e+004
1.049e+004
9.332e+003
8.168e+003
7.005e+003
5.842e+003
4.679e+003
3.516e+003
2.352e+003
1.189e+003
2.603e+001
Y
Z
X

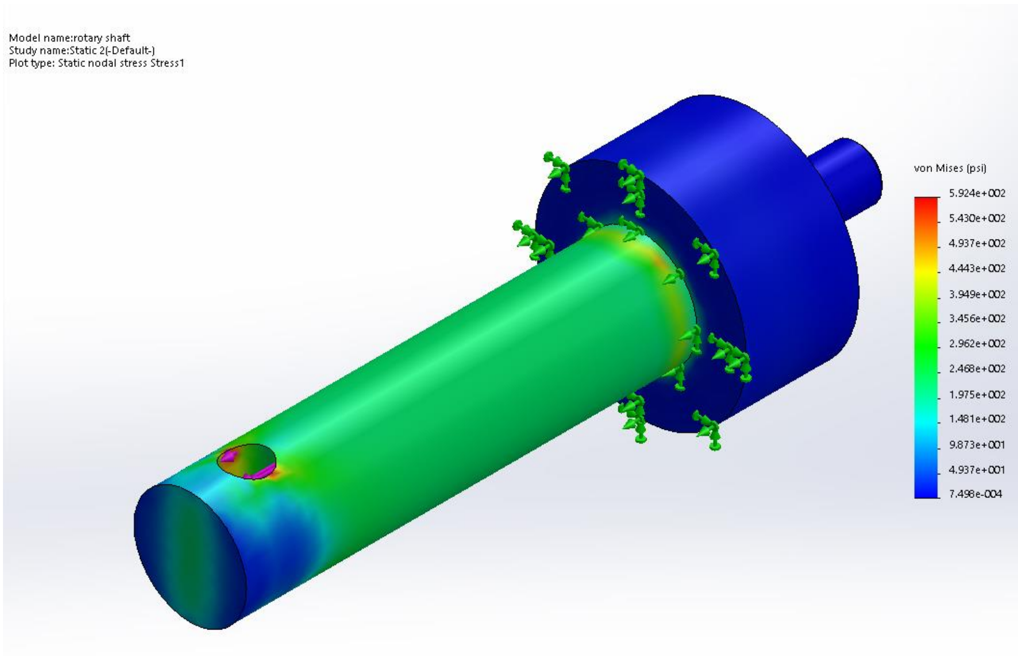
Model name:rotary shaft
Study name:Static 2(-Default-)
Plot type: Static nodal stress Stress1
von Mises (psi)
5.924e+002
5.430e+002
4.937e+002
4.443e+002
3.949e+002
3.456e+002
2.962e+002
2.468e+002
1.975e+002
1.481e+002
9.873e+001
4.937e+001
7.498e-004

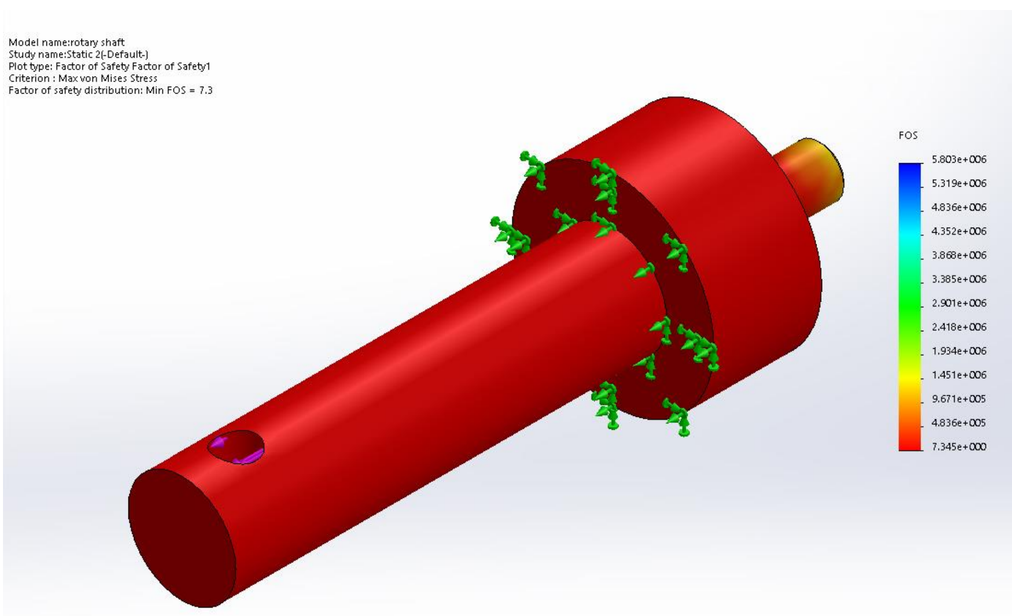
Model name:rotary shaft
Study name:Static 2(-Default-)
Plot type: Factor of Safety Factor of Safety1
Criterion : Max von Mises Stress
Factor of safety distribution: Min FOS = 7.3
FOS
5.803e+006
5.319e+006
4.836e+006
4.352e+006
3.868e+006
3.385e+006
2.901e+006
2.418e+006
1.934e+006
1.451e+006
9.671e+005
4.836e+005
7.345e+000

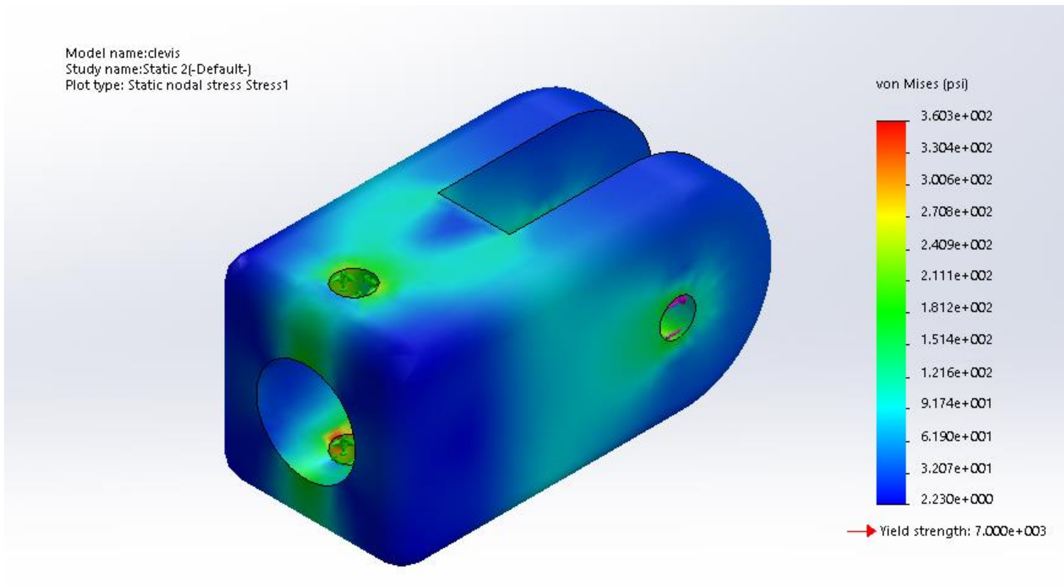
Model name:clevis
Study name:Static 2(-Default-)
Plot type: Static nodal stress Stress1
von Mises (psi)
3.603e+002
3.304e+002
3.006e+002
2.708e+002
2.409e+002
2.111e+002
1.812e+002
1.514e+002
1.216e+002
9.174e+001
6.190e+001
3.207e+001
2.230e+000
Yield strength: 7.000e+003

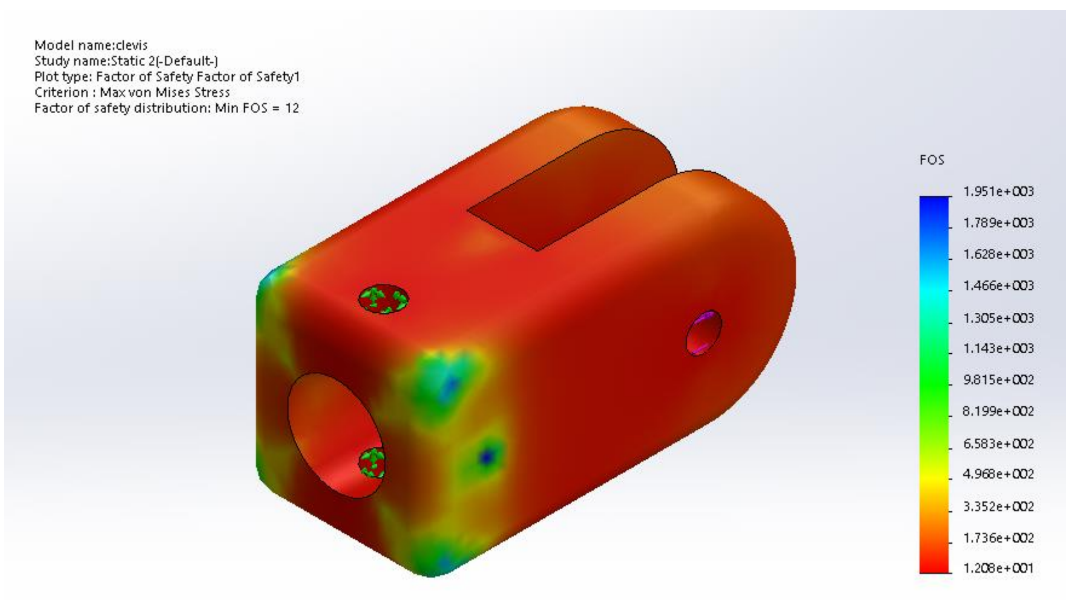
Model name:clevis
Study name:Static 2(-Default-)
Plot type: Factor of Safety Factor of Safety1
Criterion : Max von Mises Stress
Factor of safety distribution: Min FOS = 12
FOS
1.951e+003
1.789e+003
1.628e+003
1.466e+003
1.305e+003
1.143e+003
9.815e+002
8.199e+002
6.583e+002
4.968e+002
3.352e+002
1.736e+002
1.208e+001

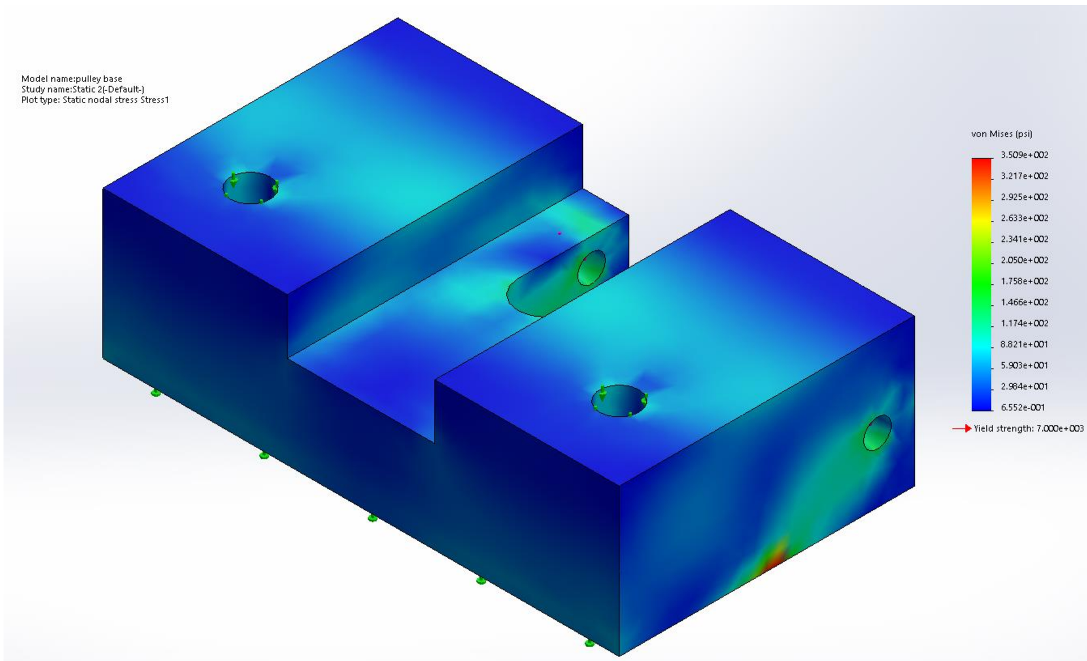
Model name:pulley base
Study name:Static 2(-Default-)
Plot type: Static nodal stress Stress1
von Mises (psi)
3.509e+002
3.217e+002
2.925e+002
2.633e+002
2.341e+002
2.050e+002
1.758e+002
1.466e+002
1.174e+002
8.821e+001
5.903e+001
2.984e+001
6.552e-001
Yield strength: 7.000e+003

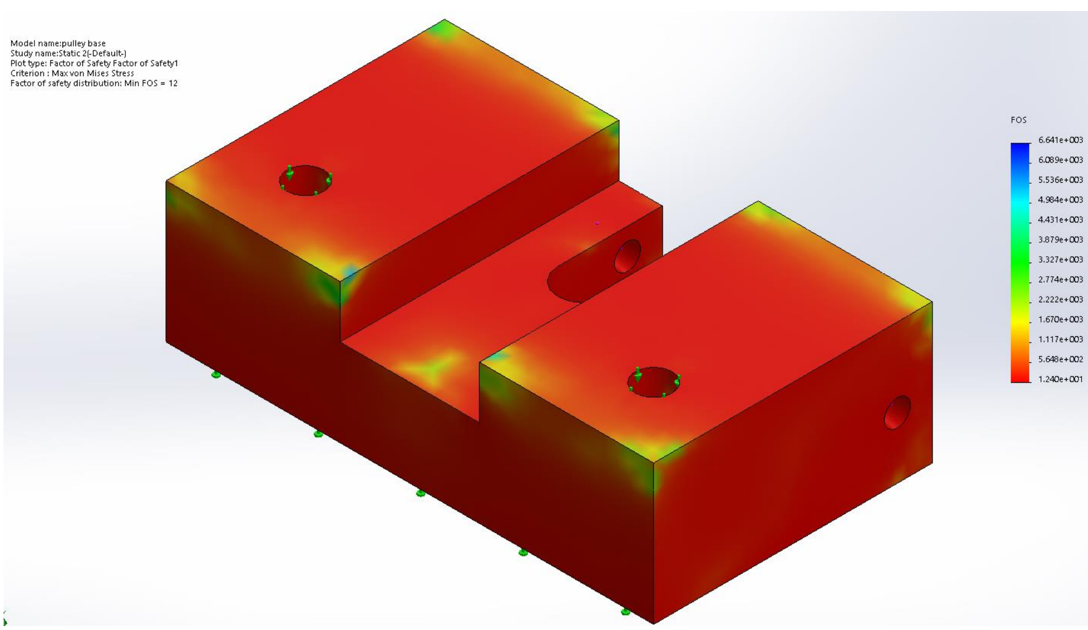
Model name:pulley base
Study name:Static 2(-Default-)
Plot type: Factor of Safety Factor of Safety1
Criterion : Max von Mises Stress
Factor of safety distribution: Min FOS = 12
FOS
6.641e+003
6.089e+003
5.536e+003
4.984e+003
4.431e+003
3.879e+003
3.327e+003
2.774e+003
2.222e+003
1.670e+003
1.117e+003
5.648e+002
1.240e+001

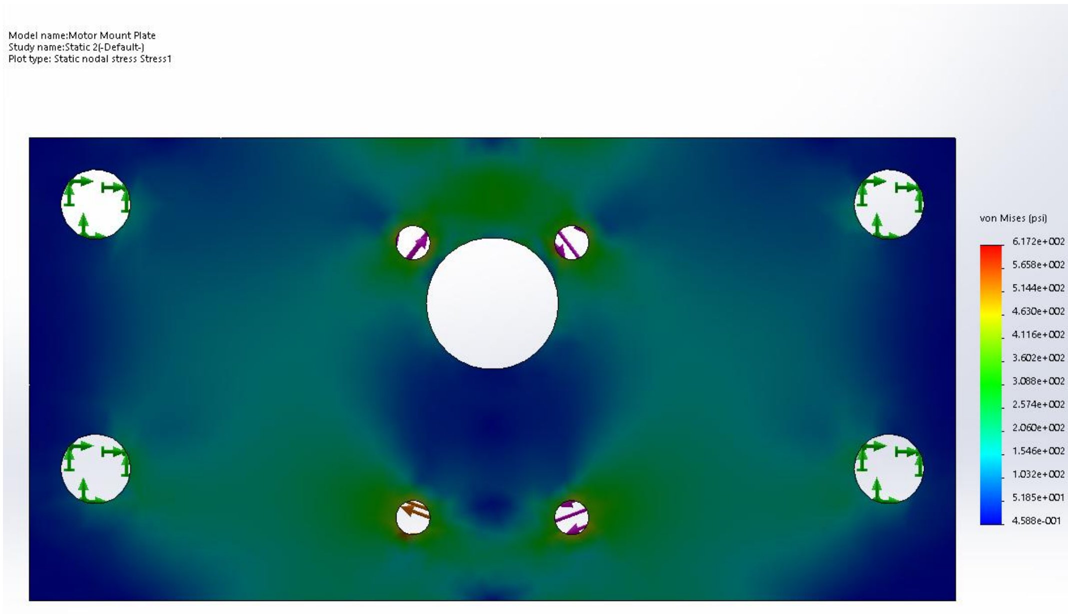
Model name:Motor Mount Plate
Study name:Static 2(-Default-)
Plot type: Static nodal stress Stress1
von Mises (psi)
6.172e+002
5.658e+002
5.144e+002
4.630e+002
4.116e+002
3.602e+002
3.088e+002
2.574e+002
2.060e+002
1.546e+002
1.032e+002
5.185e+001
4.588e-001

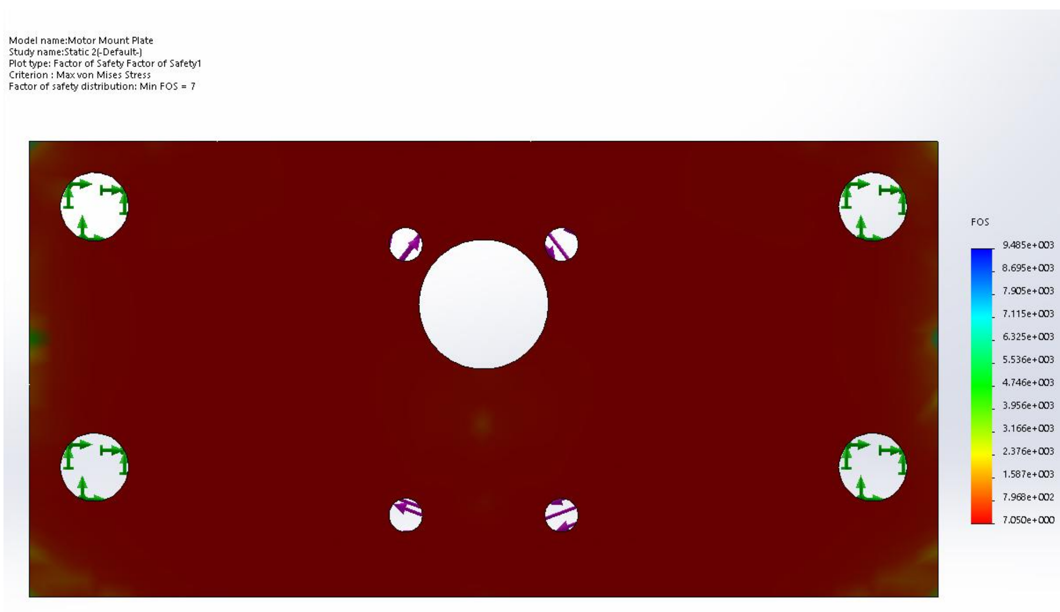
Model name:Motor Mount Plate
Study name:Static 2(-Default-)
Plot type: Factor of Safety Factor of Safety1
Criterion : Max von Mises Stress
Factor of safety distribution: Min FOS = 7
FOS
9.485e+003
8.695e+003
7.905e+003
7.115e+003
6.325e+003
5.536e+003
4.746e+003
3.956e+003
3.166e+003
2.376e+003
1.587e+003
7.968e+002
7.050e+000

Bibliography

1. *Rope User's Manual*. (2014). Retrieved from https://www.samsonrope.com
2. May, C. , Holz, B. , Wurtz, T. , Natale, C. , Palli, G. , Melchiorri, C. (2010). *Twisted String Actuation – History, Principle and Performance.* Workshop on Actuation & Sensing in Robotics. Saarbruken, Germany.
3. *Typical Engineering Properties of Polypropylene. (2014).* Retrieved from http://www.ineos-op.com
4. May, C. , Holz, B. , Wurtz, T. , Natale, C. , Palli, G. , Melchiorri, C. (2013). *Modeling and Control of the Twisted String Actuation System.* IEEE/ASME TRANSACTIONS ON MECHATRONICS, VOL. 18, NO. 2,
5. Sloan, F., Bull, S., Longerich, R. (Date not listed). *Design Modifications to Increase Fatigue Life of Fiber Ropes.* Retreived from http://www.thecortlandcompanies.com
6. Gapanov, I., Popov, D., Ryu, J. (2014). *Twisted String Actuation Systems: A Study of the Mathematical Model and a Comparison of Twisted Strings.* IEEE/ASME TRANSACTIONS ON MECHATRONICS, VOL. 19, NO. 4.
7. Tavakoli, M., Batista, R., Sgrigna, L. (2015). *The UC Softhand: Light Weight Adaptive Bionic Hand with a Compact Twisted String Actuation System.* Institute of Systems and Robotics, University of Coimbra.

8. Gapanov, I., Popov, D., Ryu, J. (2013*). Bidirectional Elbow Exoskeleton Based on Twisted-String Actuators.* Intelligent Robots and Systems.

9. Starkey, M. , Williams, R. (2011). *Capstan as a Mechanical Amplifier*. Proceedings of the ASME 2011 International Design Engineering Technical Conferences & Computers and Information in Engineering Conference